Lithuanian Journal of Physics, Vol. **60**, No. 3, pp. 194–204 (2020)

THE FORMATION OF SELF-ASSEMBLED STRUCTURES OF C_{60} IN SOLUTION AND IN THE VOLUME OF AN EVAPORATING DROP OF A COLLOIDAL SOLUTION

U.K. Makhmanov [a], A.M. Kokhkharov [a], S.A. Bakhramov [a], and D. Erts [b]

[a] *Institute of Ion-Plasma and Laser Technologies, Uzbekistan Academy Sciences, 33 Durmon Yuli St., 100125 Tashkent, Uzbekistan*

[b] *Institute of Chemical Physics, University of Latvia, 19 Raina Blvd., 1586 Riga, Latvia*

Email: urolmakh@gmail.com

Received 15 April 2020; revised 12 June 2020; accepted 17 June 2020

The results of experiments on the self-aggregation of C_{60} fullerene molecules both inside a two-component solvent (xylene/tetrahydrofuran) and in the volume of an evaporating drop of C_{60} colloidal solution on a flat substrate surface are presented. The investigations of C_{60} solutions using dynamic light scattering, transmission electron microscopy and UV–Vis absorption spectroscopy methods revealed the possibility of synthesis of fractal nanoaggregates with a diameter of up to ~135 nm at low concentrations of C_{60} in the solutions. The final geometric dimensions of C_{60} nanoaggregates were determined by the initial concentration of fullerene in the solvent medium. Using the scanning electron microscopy method, we have shown that in an open dissipative system – in the volume of an evaporating droplet of the colloidal solution of fullerene C_{60} sessile on the surface of a flat glass substrate, large quasispherical nanoaggregates with an average diameter of ~380–800 nm are formed. The physical features and regularities that characterize the processes of self-aggregation of fullerene particles in the volume of a drying drop were determined.

Keywords: fullerene C_{60}, solvent mixture, self-aggregation, nanoaggregate, evaporating drop

PACS: 61.46.Bc, 81.05.Tp

1. Introduction

The fullerene C_{60} molecule (icosahedral I_h symmetry), consisting of 60 sp^2-bonded carbon atoms, is a completely organic macromolecule of spherical shape with a diameter of $d_0 \approx 0.714$ nm. High polarizability, strong electron-acceptor activity and hydrophobicity are main unique properties of fullerene C_{60}. Unlike other well-known allotropic forms of carbon, fullerene C_{60} is well soluble in the vast majority of low-polarity organic solvents (for example, benzene, toluene, xylene, carbon disulfide, tetralin, and others), but practically insoluble in polar solvents such as alcohols [1, 2].

In a number of pure and mixed organic solvents, fullerene C_n (n = 60, 70, 76, …) molecules show a pronounced tendency to self-assembly and the formation of fairly large functional fullerene aggregates of various shapes and sizes. The problem was fundamentally studied by different physical and chemical methods in [3–11] and the obtained results provided a vector toward potential applications in material chemistry [12, 13], biomedicine [14–16], phototherapy [17–19], molecular electronics [20], optoelectronics [21, 22] and solar energy [23–25].

In recent years, the interest of researchers to the processes occurring during the drying of liquid droplets (in particular, nanoparticle solutions) on a flat substrate has increased significantly [26–30]. The process of drying up a drop of solutions attracts the attention of physicists and technologists

as a natural model of a self-organizing system in which the variation in the type of a solute or solvent, in substrate type and its initial thermodynamic parameters leads to interesting physical phenomena taking place [31–34]. The interest is determined also by the need for improving the technologies associated with these processes, for example, low-cost synthesis of organic solar cells [35, 36], as an auxiliary criterion in medical diagnostics [37–39], as a new direct-writing printing technique by applying paint coatings on various surfaces [40, 41], as a technique to fabricate ordered arrays of structures in nanosphere lithography [42, 43].

It should be noted that the physical foundations and mechanisms of self-aggregation processes of nanoparticles in solutions and in drying drops of nanoparticle solutions (in particular, solutions of fullerene C_{60} in two-component organic solvents) on a flat substrate are still not fully understood, which complicates the transition to effective management of nanomaterial production processes.

The purpose of this work is an experimental study of the self-aggregation of C_{60} fullerene molecules both inside the solution and in the volume of an evaporating drop of C_{60} colloidal solution sitting on the flat surface of a substrate.

2. Samples and techniques

To prepare initial molecular solutions of C_{60}, we used dry crystalline powders of fullerene C_{60} of high purification (>99.8% of the base material, manufacturer *SES Research*, USA) as well as organic solvents – xylene (C_8H_{10}) and tetrahydrofuran (C_4H_8O) with 99.9% purity (*Sigma-Aldrich*, USA). The solvents were used as received. The maximum fullerene C_{60} solubility at room temperature in pure xylene is about 7.2 mol/m^3 and in pure tetrahydrofuran (THF) it is about 0.083 mol/m^3. A special standard cover glass (*ISOLAB Laborgerate GmbH*, Germany) was used as a substrate.

The initial fullerene working solutions were prepared in a dark room by the nonequilibrium method described in paper [44].

The structure of synthesized nanostructures of fullerene C_{60} was characterized by a transmission electron microscope (TEM) LEO-912 AB (*ZEISS*, Germany) and a field emission scanning electron microscope (SEM) *Hitachi* S-4800 (Japan). In the experiments to study the evolution of distribution of fullerene C_{60} molecules and the formation of ring structures of mC_{60} nanoaggregates (where m is the number of C_{60} molecules in a synthesized nanoaggregate) on the surface of a glass substrate, we used an optical binocular microscope of the brand *Motic* B1-220A (Germany) with a digital camera for continuous recording of images.

The size distribution of C_{60} fullerene nanoaggregates in the solutions was studied by dynamic light scattering (DLS). The DLS measurements were performed on a Zetasizer Nano ZEN3600 (*Malvern Instruments Ltd.*) equipped with a He-Ne laser (4 mW at 632.8 nm) at room temperature ($T \approx 24\pm1$°C).

The electronic absorption spectra of C_{60} solutions in two-component organic solvents (which were used in 'drop drying' experiments) were recorded on a *Shimadzu* UV-2700 UV–Vis recording spectrometer (*Shimadzu*, Japan) with a high spectral resolution (~0.1 nm) using a 1 cm thick quartz cuvette.

Before each series of experiments, the surface of the used glass substrate was thoroughly plasma cleaned using a Plasma Cleaner device of the PDC-002 brand (*Harrick Plasma Inc*, USA). Droplets of the colloidal solution of C_{60} were placed using a VITLAB piston-operated micropipette (*VITLAB GmbH*, Germany) on the previously cleaned surface of a strictly horizontal mounted flat glass substrate. The shape of the initial droplets of C_{60} solutions on the flat substrate is approximately described by a spherical cap. Complete evaporation of the solvent from the droplet takes place in a laboratory box at a temperature of ~24±1°C and a relative humidity of ~40–45%. Drops of C_{60} during the evaporation were protected against convective air flows.

3. Results and discussion

Figure 1 shows the DLS experiment of the distribution of light scattering particles according to their hydrodynamic diameters at two different concentrations of C_{60} in a fresh solution prepared by the non-equilibrium method in a mixture of two organic solvents – xylene and THF at a volume fraction of 0.95:0.05, respectively. At a C_{60} concentration of ~0.312 mol/m^3, the main fraction of light-scattering fullerene nanoparticles in the solution is distributed in the diameter range ~3.5–63.2 nm and the maximum distribution of C_{60} fullerene aggregates is localized in the region of ~12.86 nm

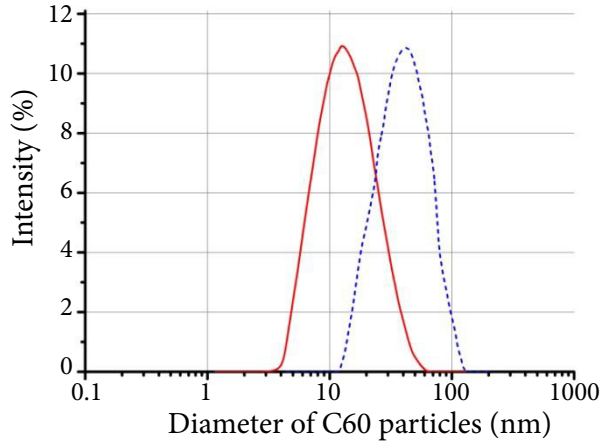

Fig. 1. The size distribution of mC_{60} nanoaggregates in the freshly prepared fullerene solution in the xylene/THF mixture by light intensity at two different solute concentrations: 0.312 (a solid line) and 0.468 mol/m^3 (a dashed line).

(a solid line). The mean hydrodynamic diameter of light scattering fullerene particles at a relatively high concentration of C_{60} (~0.468 mol/m^3) shifts to ~41.9 nm and the hydrodynamic size range of mC_{60} nanoaggregates corresponds to ~11.7–135.0 nm (a dashed line). The obtained DLS results show that the used C_{60} solutions belong to the dispersed colloidal system and the synthesis of mC_{60} nanoaggregates in xylene/THF mixtures occurs almost immediately after the preparation of the solution. During the self-assembly of fullerene molecules in a nonequilibrium solution, C_{60} molecules form a nanostructure, finding the most advantageous combination of interactions between molecules with minimal free energy [45, 46]. In this process, a higher initial solute concentration in the solution leads to a greater number of iterations (repetitions) of the self-assembly of C_{60} molecules. The latter plays an important role in the synthesis of large mC_{60} nanoaggregates in the solution (Fig. 1, a dashed line).

Figure 2 represents a TEM image of the nanosized mC_{60} aggregates synthesized in the freshly prepared solution of C_{60} in a xylene/THF mixture with a volume fraction of 0.95:0.05, respectively, at a solute concentration of ~0.468 mol/m^3. The TEM image of the synthesized mC_{60} nanoaggregates inside the C_{60} solution is obtained by rapid freezing (~1270 K/s) of a thin layer of the drop of the working solution of C_{60} fullerene with liquid nitrogen vapours using a special automated device Vitrification Robot FP 5350/62 (*ZEISS*, Germany). It can be seen that there are also small nanoaggregates with diameters up to ~30 nm, and large mC_{60} nanoaggregates with diameters up to ~135 nm with porous structures containing discrete intermediate small nanoaggregates.

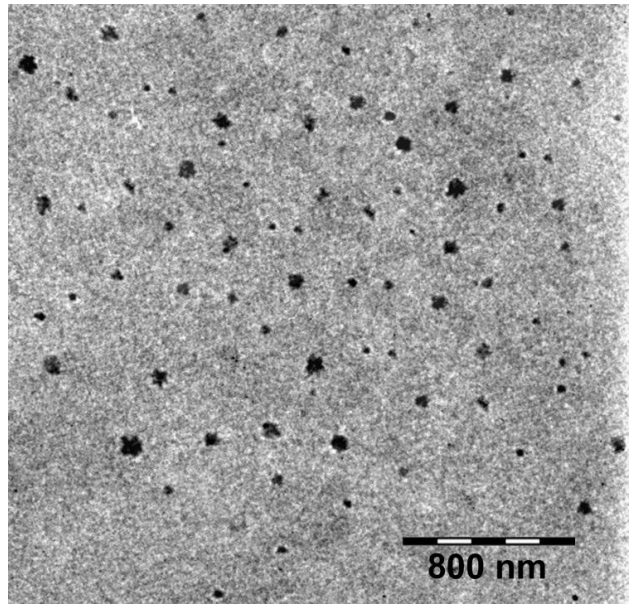

Fig. 2. TEM image of the nanosized C_{60} aggregates synthesized in the freshly prepared solution of C_{60} fullerene in two-component organic solvents (xylene and THF with a volume fraction of 0.95:0.05, respectively).

For the mC_{60} nanoaggregates with a C_{60} concentration of ~0.468 mol/m^3 the agreement between the TEM result and the DLS data is excellent. Note that earlier we studied [44] the self-aggregation of fullerene C_{60} molecules in a toluene/THF mixture with a volume fraction of 0.9:0.1, respectively. In [44], it was found that it was possible to synthesize larger porous spherical mC_{60} aggregates with a diameter of ~700 nm in a nonequilibrium solution.

Figure 3 shows the UV–Vis absorption spectra of freshly prepared working solutions of fullerene C_{60} at lower onset concentrations of C_{60}. With an increase in the concentration of fullerene, the intense absorption band for molecular C_{60} with a maximum at $\lambda_1 \approx 336.1$ nm, corresponding to the symmetry-allowed $1^1A_g \rightarrow 3^1T_{1u}$ transition, expands and does exhibit a small positive solvatochromism effect (~2 nm). This is due to the processes of intermolecular dipole–dipole π~π^* stacking interactions 'C_{60}–solvents' that control the formation and further growth of the mC_{60}

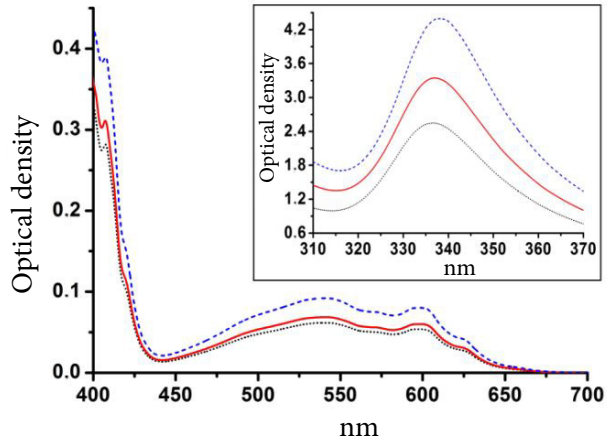

Fig. 3. The absorption spectra of freshly prepared solutions of fullerene C_{60} in xylene and THF mixtures with a volume fraction of 0.95:0.05, respectively, at a various initial concentration of C_{60}: 0.208 (a dotted line), 0.312 (a solid line) and 0.468 mol/m^3 (a dashed line). The inset shows the ~336 nm band of C_{60} in the solution with the above concentration.

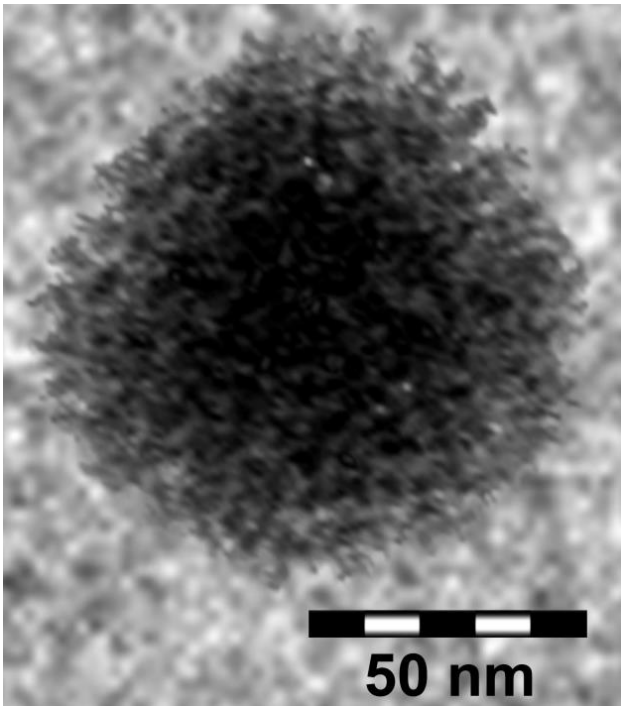

Fig. 4. HRTEM image of the fractal mC_{60} nanoaggregate, synthesized in the fresh non-equilibrium solution of C_{60} fullerene in the xylene/THF mixture with a volume fraction of 0.95:0.05, respectively.

nanoaggregates [47]. It should be noted that in the experiments, an increasing concentration of C_{60} monomers in the solution leads to overcome interactions between 'C_{60}–solvents' molecules and to increase the van der Waals interaction between 'C_{60}–C_{60}'. The narrow absorption band of C_{60} with a maximum at $\lambda_2 \approx 407.5$ nm (corresponds to the symmetry-allowed $1^1A_g \rightarrow 1^1T_{1u}$ transition) and the broad optical absorption bands with maxima at $\lambda_3 \approx 540.6$ nm ($S_1 \rightarrow S_3$ transition), $\lambda_4 \approx 598.4$ nm ($S_0 \rightarrow S_1$) and $\lambda_5 \approx 624.8$ nm ($h_u \rightarrow t_{1u} + T_u$) are also observed in the spectrum. With increasing the used concentration of C_{60} in the fresh solution, the amplitudes of these characteristic optical absorption bands in the spectrum increase unevenly. The latter are attributed to the formation of mC_{60} nanoaggregates in the solution due to the charge transfer between C_{60} and C_{60} resulting from electronic transitions HOMO–LUMO. Changes in the optical absorption spectra of C_{60} solutions indicate that the formation of mC_{60} aggregates in the solution begins directly in the process of its preparation.

Figure 4 shows a HRTEM image of the porous mC_{60} nanoaggregate that indeed suggests a fractal character. The self-aggregation of C_{60} molecules and the formation of nanostructured porous fractal aggregates in the initial solution of fullerene (with a solvent concentration of ~0.468 mol/m^3), in our opinion, will occur according to the following mechanism. It is known [45, 46, 48] that the minimum free energy of the C_{60}/'low polar solvent' system can only be achieved by forming the initial stable aggregate with a diameter of ~4.6 nm containing 55 molecules of C_{60}.

In our experiments, firstly, under the additional influence on C_{60} molecules of the rotational diffusion of molecules in the initial non-equilibrium solution and their chaotic diffusion motion, primary spherical mC_{60} clusters containing $m = 55$ fullerene molecules are synthesized. Then this procedure of self-aggregation in the solution is repeated many times in accordance with the 'cluster–cluster' aggregation model, which over time increases the characteristic size of the clusters and reduces their number. This is possible to ensure the predictability of the dimensional, structural and weight characteristics of mC_{60} nanoaggregates synthesized in experiments.

Under similarity conditions of the aggregation of C_{60} particles, the fractal dimension of mC_{60} nanoaggregate may be represented by the formula [46]

$$D = \frac{\ln m}{\ln d - \ln d_0}, \quad (1)$$

where m is the number of C_{60} molecules in the synthesized nanoaggregate, d is the diameter of the nanoaggregate, and d_0 is the diameter of an individual C_{60} macromolecule.

Using Eq. (1) and values of m = 55, d = 4.6 nm and d_0 = 0.714 nm, we found that the fractal dimension of the synthesized mC_{60} aggregate in the solution is $D \approx 2.148$. Our calculations allowed us to establish that one synthesized fractal nanoaggregate mC_{60}, in the centre of which one of the C_{60} molecules is located, and having a diameter of ~100 nm can contain up to $m \approx 40762$ individual C_{60} molecules (see Fig. 4).

Figure 5 shows a schematic representation of the circulation flows (a) leading to the self-assembly of fullerene C_{60} particles in a variable volume of a drop and a photograph of an isolated drop of a fullerene C_{60} solution lying on the surface of a glass substrate (b).

In the process of conducting experimental studies of the features of evaporation of droplets set on the surface of a horizontally installed flat glass substrate, and containing both pure organic solvent and solutions of fullerene C_{60} in an organic solvent, we found the following basic patterns of the behaviour of a drop:

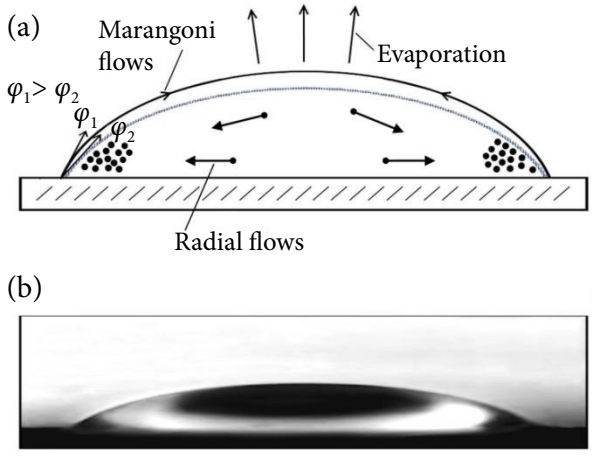

Fig. 5. (a) A schematic representation of the appearing flows inside the evaporating droplet and (b) a photograph of the lateral microdroplet profiles of a colloidal C_{60} solution with a base diameter of ~7 mm lying on the surface of a glass substrate. The arrow inside the droplet and on the droplet–air interface line shows the direction of the radial and Marangoni flows, respectively. The direction of evaporation of the solvent from the droplet is orthogonal to the tangent plane at each point of the droplet surface.

(i) Droplets taken from pure organic solvents (xylene or THF), throughout thermal evaporation, always keep the contact angle φ (see Fig. 5(a)) and their evaporation rate is not identical; however, there is a gradual narrowing of the base area of the 'drop–glass substrate' contact until the drop completely disappears;

(ii) If a drop of a mixture of organic solvents (xylene/THF) contains colloidal particles of a solute, for example, fullerene C_{60} (see Fig. 5(b)), then a fundamentally different picture is realized – as the thermal evaporation of solvents from the drop occurs, the base of the drop remains constant and the 'pinning' mode of the contact line is realized. The edge angle of the droplet gradually decreases up to $\varphi \approx 0°$. In this case, due to the influence of Marangoni effects [49] in near-surface layers of the evaporating drop of the C_{60} solution, strong capillary flows arise (the so-called Marangoni flows). During evaporation, binary organic solvents with different volatility and surface tension from a sessile droplet cause radial convection inside the droplet. The latter directly initiates the mutual approach of C_{60} colloidal particles and the synthesis of large mC_{60} aggregates.

Figure 6 shows the evolution of ring formation during the thermal evaporation of a sessile C_{60} drop on the surface of a glass substrate. In the figures, the evaporation process continues in the sequence a–b–c–d. The time of complete evaporation of xylene and THF from the volume of microdrop (~40 μl) at room temperature was ~2 h. Obviously, after the completion of natural thermal evaporation of the organic solvents from the droplet of colloidal C_{60} solution (initial fullerene concentration of ~0.468 mol/m^3), non-concentric ring-shaped structures were found on the surface of the glass substrate (see Fig. 6), the occurrence of which can be explained only by self-assembly of colloidal fullerene particles in the process of evaporation of a solution drop and the formation of large mC_{60} aggregates in different sizes.

One of the main driving forces that initiate the self-aggregation of particles C_{60} is the evaporation of solvents (xylene/THF) and the associated change in the volume of the droplet. In this case, strong capillary forces in the border (in the near

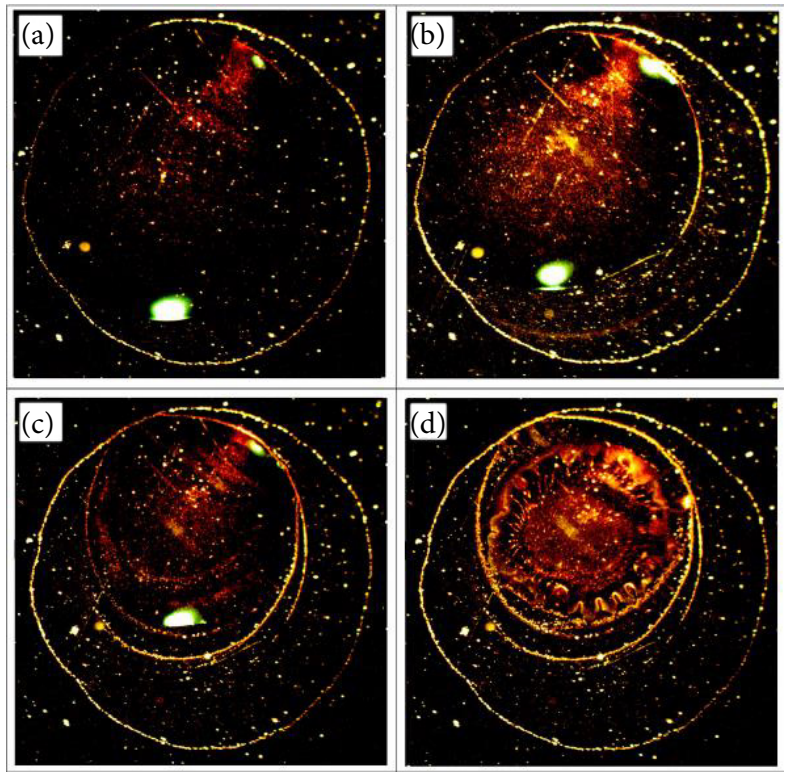

Fig. 6. The evolution of distribution of fullerene C_{60} particles and formation of a non-concentric ring consisting of mC_{60} nanosized aggregates on the surface of a glass substrate in the process of thermal evaporation of organic solvents (xylene and THF at a volume fraction of 0.95:0.05, respectively) at room temperature from the C_{60} solution droplet with a volume of $V \approx 40$ μl.

surface layers) of the droplet and the radial convection inside the droplet lead to motion and shifting of particles of fullerene C_{60} from the bulk of the droplet to the periphery. The key result is that part of the aggregated particles of C_{60} is deposited and ultimately leads to the formation of a ring stain (see Fig. 6). Self-aggregation is a collective process in which the whole ensemble of fullerene C_{60} nanoparticles participates. It is not difficult to see that the C_{60} nanoparticles, which did not participate in the synthesis of initial mC_{60} nanoaggregates, as the droplets evaporated, moved further along the surface of the glass substrate together with the organic solvents.

Next, we investigated the location and distribution of the synthesized mC_{60} aggregates inside and outside the ring by a scanning electron microscope. Figure 7 shows a two-dimensional SEM image of small arbitrarily selected areas inside the rings, shown in Fig. 6. It can be seen that after the complete evaporation of xylene and THF from a microdroplet of the colloidal C_{60} solution on the surface of the optical glass substrate large mC_{60} aggregates of a quasispherical shape were aggregated. The beginning of each ring contains relatively large mC_{60} aggregates. The space between the two rings is covered with layers of small mC_{60} aggregates.

Figure 8 presents a SEM image of mC_{60} aggregates synthesized during the thermal evaporation of organic solvents from the volume of microdrops of a C_{60} colloidal solution on the surface of a substrate. It can be seen that the average geometric dimensions in the diameter of mC_{60} aggregates vary in a range of ~380÷800 nm. The formed mC_{60} aggregates consist of discrete intermediate nanoaggregates with sizes in diameter up to ~135 nm (see Fig. 8(a)). This size corresponds with the diameter of the aggregates that were synthesized inside the colloidal solutions of fullerene C_{60}. Other than that, most of the mC_{60} structures formed have a pipe-like structure consisting of several layers (see Fig. 8(b)).

In our opinion, a droplet of the colloidal solution of C_{60} in an organic solvent, as well as a drop

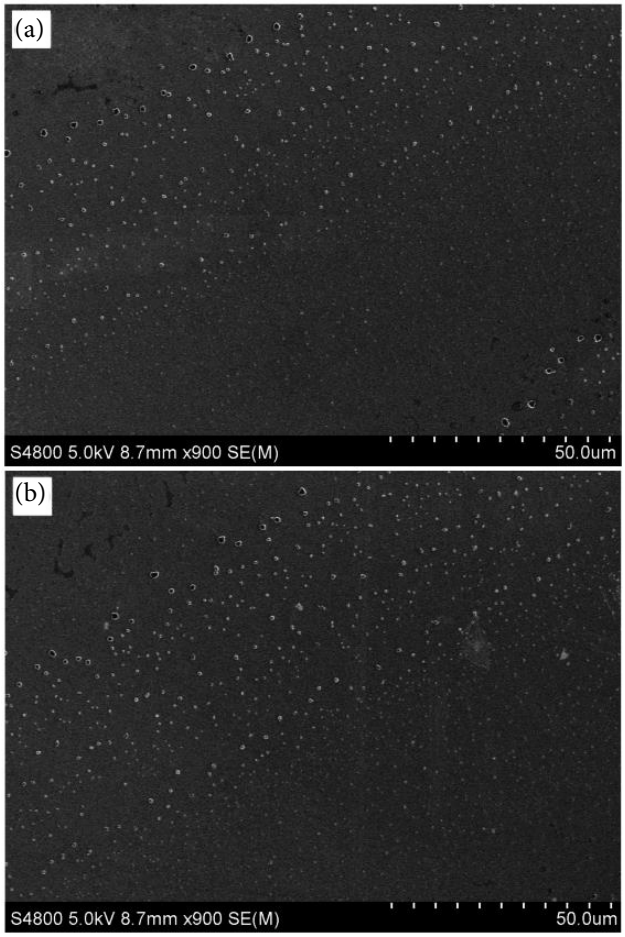

Fig. 7. SEM image of the arrangement of mC_{60} aggregates in the contact line sections after the complete evaporation of organic solvents from a volume drop of the colloidal solution of fullerene C_{60} on the planar surface of a glass substrate. The centre of the drop lies at the bottom right side of the image.

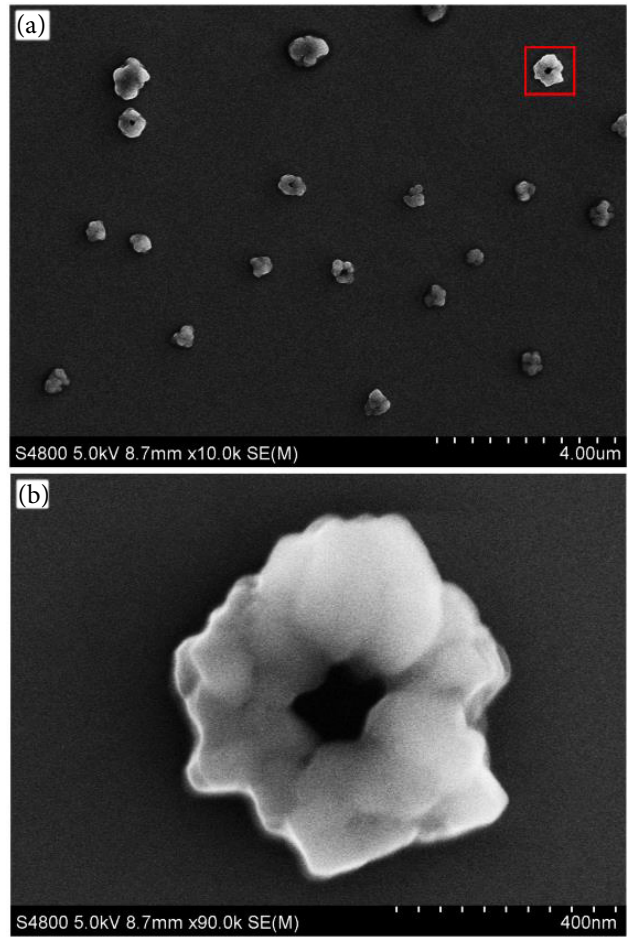

Fig. 8. SEM image of the mC_{60} aggregates formed by a thermal evaporation mixture of organic solvents (xylene and THF with a volume fraction of 0.95:0.05, respectively) from the volume of a microdroplet of the C_{60} colloidal solution on the substrate surface and (b) magnification of the area inside the box in (a). The initial concentration of fullerene C_{60} in the solution was ~0.468 mol/m^3.

of the solution of any other nanoparticles, always seek to minimize their total surface energy. The latter can be achieved, in particular, as a result of self-aggregation of solute particles. Suppose that two intermediate fullerene clusters with diameters d_1 and d_2 (where $d_1 \ll d_2$) are localized in the volume of an evaporating drop of the C_{60} solution. Then, each of these nanoscale particles under consideration will tend to establish a thermodynamic equilibrium with the solution surrounding it. So, smaller particles with a diameter d_1 in a droplet will be deposited on the surface of clusters with a diameter d_2 that are larger in size to maintain the equilibrium in the system. As a result of this self-assembly of fullerene particles in the volume of evaporating droplets, large mC_{60} nanoaggregates grow in size even more (up to ~800 nm in diameter).

Thus, our experimental results on the study of the evaporation of individual drops of a fullerene C_{60} colloidal solution on the surface of a substrate will be very useful in solving the problems of evaporating limited volumes of nanoparticle liquids in various technological devices, for the further development of technologies for applying thin semiconductor coatings, etc.

4. Conclusions

We have investigated the self-aggregation of C_{60} fullerene molecules both inside the freshly prepared solution and in the volume of an evaporating drop of the C_{60} colloidal solution. In the non-equilibrium

solutions of fullerene C_{60} in the xylene/THF mixture (prepared by continuous stirring of the solution on a magnetic stirrer) at room temperature, large quasispherical mC_{60} nanoaggregates with a diameter of up to ~135 nm having a porous structure with fractal dimension $D \approx 2.148$ were synthesized. The finite geometrical sizes of the mC_{60} nanoaggregates are determined by the initial concentration of C_{60} in the used solvent medium. The results obtained on the self-aggregation of C_{60} molecules in the xylene/THF solution were confirmed by DLS, TEM and optical absorption studies.

After the completion of natural thermal evaporation of the organic solvent (xylene/THF) from a droplet of the colloidal C_{60} solution, non-concentric ring-shaped structures were found on the standard substrate surface, the occurrence of which may be explained by the self-assembly of colloidal particles of fullerene. As a result, nanostructured and porous mC_{60} aggregates of large geometrical sizes (up to ~800 nm in diameter) were synthesized on the substrate surface. In turn, finite mC_{60} nanoaggregates consist of smaller intermediate discrete C_{60} aggregates with geometrical sizes in diameter up to ~135 nm. Prolonged (within three months) microscopic observations of the state of the synthesized mC_{60} aggregates on a glass surface allowed us to conclude that they have a high structural stability.

The experimentally obtained results on the formation of porous nanostructured mC_{60} aggregates in a freshly prepared solution and from a drying microdroplet of the colloidal solution of C_{60} apparently open up some new possibilities of producing new nanosized functional materials/thin films for micro- and optoelectronics, solar batteries, power electronics, biochips and other areas of semiconductor technology.

Aknowledgements

This research was supported by the Foundation for Basic Research of the Academy of Sciences of Uzbekistan: 'Fundamental Foundations for the Synthesis of New Functional Nanomaterials for Optoelectronics and Solar Energy Based on Fullerenes and Their Derivatives' (Project No. OT-F2-51). We are very grateful to the Government of Latvia for providing a research scholarship and assistance in completing a scientific internship at the Institute of Chemical Physics of the University of Latvia.

References

[1] K.N. Semenov, N.A. Charykov, V.A. Keskinov, A.K. Piartman, A.A. Blokhin, and A.A. Kopyrin, Solubility of light fullerenes in organic solvents, J. Chem. Eng. Data **55**, 13 (2010), https://doi.org/10.1021/je900296s

[2] N.O. Mchedlov-Petrossyan, Fullerenes in molecular liquids. Solutions in 'good' solvents: Another view, J. Mol. Liq. **161**, 1 (2011), https://doi.org/10.1016/j.molliq.2011.04.001

[3] I.I. Adamenko, L.A. Bulavin, K.O. Moroz, and I.Yu Prilutski, Equation of state for C_{60} toluene solution, J. Mol. Liq. **105**, 149 (2003), https://doi.org/10.1007/s10765-005-5578-2

[4] K.L. Chen and M. Elimelech, Aggregation and deposition kinetics of fullerene (C_{60}) nanoparticles, Langmuir **22**, 10994 (2006), https://doi.org/10.1021/la062072v

[5] A.J. Patnaik, Structure and dynamics in self-organized C_{60} fullerenes, Nanosci. Nanotechnol. **7**, 1111 (2007), https://doi.org/10.1166/jnn.2007.303

[6] N.O. Mchedlov-Petrossyan, Fullerenes in liquid media: an unsettling intrusion into the solution chemistry, Chem. Rev. **113**, 5149 (2013), https://doi.org/10.1021/cr3005026

[7] A.M. Kokhkharov, E.A. Zakhidov, Sh.P. Gofurov, S.A. Bakhramov, and U.K. Makhmanov, Clusterization of fullerene C_{70} molecules in solutions and its influence to optical and nonlinear optical properties of solutions, Int. J. Nanosci. **12**, 1350027 (2013), https://doi.org/10.1142/S0219581X13500270

[8] A. Ruiz, M. Suarez, N. Martin, F. Albericio, and H. Rodríguez, Morphological characterization of fullerene–androsterone conjugates, Beilstein J. Nanotechnol. **5**, 374 (2014), https://doi.org/10.3762/bjnano.5.43

[9] S.A. Bakhramov, A.M. Kokhkharov, E.A. Zakhidov, U.K. Makhmanov, and S.P. Gofurov, Clusterization of fullerene $C_{60/70}$ molecules in solutions and its influence on the optical and the nonlinear optical properties of solutions, J. Korean Phys. Soc. **64**, 1494 (2014), https://doi.org/10.3938/jkps.64.1494

[10] T.V. Nagorna, O.A. Kyzyma, D. Chudoba, and A.V. Nagornyi, Temporal solvatochromic effect in

ternary C_{70}/toluene/N-methyl-pyrrolidine-2-one solution, J. Mol. Liq. **235**, 111 (2017), https://doi.org/10.1016/j.molliq.2016.12.017

[11] N.S. Lebedeva, Y.A. Gubarev, A.M. Kolker, and N.Y. Borovkov, Thermochemical insights into fullerene aggregation and the phthalocyanine-fullerene interaction in efficient solvents, ChemPhysChem **19**, 284 (2018), https://doi.org/10.1002/cphc.201701127

[12] N. Tagmatarchis and H. Shinohara, Fullerenes in medicinal chemistry and their biological applications, Mini-Rev. Med. Chem. **1**, 339 (2001), https://doi.org/10.2174/1389557013406684

[13] B. Sitharaman, T.Y. Zakharian, A. Saraf, P.M. J. Ashcroft, S. Pan, Q.P. Pham, A.G. Mikos, L.J. Wilson, and D.A. Engler, Water-soluble fullerene (C_{60}) derivatives as nonviral gene-delivery vectors, Mol. Pharm. **5**, 567 (2008), https://doi.org/10.1021/mp700106w

[14] J. Tam, J. Liu, and Z. Yao, Effect of microstructure on the antioxidant properties of fullerene polymer solutions, RSC Adv. **3**, 4622 (2013), https://doi.org/10.1039/C3RA22582H

[15] J.D. Fortner, D.Y. Lyon, C.M. Sayes, A.M. Boyd, J.C. Falkner, E.M. Hotze, L.B. Alemany, Y.J. Tao, W. Guo, K.D. Ausman, V.L. Colvin, and J.B. Hughes, C_{60} in water: nanocrystal formation and microbial response, Environ. Sci. Technol. **39**, 4307 (2005), https://doi.org/10.1021/es048099n

[16] D.Y. Lyon, L.K. Adams, J.C. Falkner, and P.J.J. Alvarez, Antibacterial activity of fullerene water suspensions: effects of preparation method and particle size, Environ. Sci. Technol. **40**, 4360 (2006), https://doi.org/10.1021/es0603655

[17] S.R. Grobmyer and V. Krishna, Minimally invasive cancer therapy using polyhydroxy fullerenes, Eur. J. Radiol. **81**, S51 (2012), https://doi.org/10.1016/S0720-048X(12)70019-0

[18] S. Kim, D.J. Lee, D.S. Kwag, U.Y. Lee, Y.S. Youn, and E.S. Lee, Acid pH-activated glycol chitosan/fullerene nanogels for efficient tumor therapy, Carbohyd. Polym. **101**, 692 (2014), https://doi.org/10.1016/j.carbpol.2013.09.108

[19] Q. Li, C. Liu, and H.J. Li, Induction of endogenous reactive oxygen species in mitochondria by fullerene-based photodynamic therapy, Nanosci. Nanotechnol. **16**, 5592 (2016), https://doi.org/10.1166/jnn.2016.11717

[20] N. Furuuchi, R. Shrestha, Y. Yamashita, T. Hirao, K. Ariga, and L. Shrestha, Self-assembled fullerene crystals as excellent aromatic vapor sensors, Sensors **19**, 267 (2019), https://doi.org/10.3390/s19020267

[21] Y. Shen, A. Saeki, S. Seki, J.-O. Lee, J. Aimi, and T. Nakanishi, Exfoliation of graphene and assembly formation with alkylated-C_{60}: a nanocarbon hybrid towards photo-energy conversion electrode devices, Adv. Opt. Mater. **3**, 925 (2015), https://doi.org/10.1002/adom.201400619

[22] S. Das and M.J. Presselt, Progress and development in structural and optoelectronic tunability of supramolecular nonbonded fullerene assemblies, Mater. Chem. C **7**, 6194 (2019), https://doi.org/10.1039/C9TC00889F

[23] S. Das, F. Herrmann-Westendorf, F.H. Schacher, E. Täuscher, U. Ritter, B. Dietzek, and M. Presselt, Controlling electronic transitions in fullerene van der Waals aggregates via supramolecular assembly, ACS Appl. Mater. Interfaces **8**, 21512 (2016), https://doi.org/10.1021%2Facsami.6b06800

[24] C. Lindqvist, E. Moons, and J. Stam, Fullerene aggregation in thin films of polymer blends for solar cell applications, Materials **11**, 2068 (2018), https://doi.org/10.3390/ma11112068

[25] Y. Mao, W. Li, M. Chen, X. Chen, R.S. Gurney, and D. Liu, Evolution of molecular aggregation in bar-coated non-fullerene organic solar cells, Mater. Chem. Front. **3**, 1062 (2019), https://doi.org/10.1039/C9QM00078J

[26] T.P. Bigioni, X.M. Lin, T.T. Nguyen, E.I. Corwin, T.A. Witten, and H.M. Jaeger, Kinetically driven self assembly of highly ordered nanoparticle monolayers, Nat. Mater. **5**, 265 (2006), https://doi.org/10.1038/nmat1611

[27] M. Nuzzo, A. Millqvist-Fureby, J. Sloth, and B. Bergenstahl, Surface composition and morphology of particles dried individually and by spray drying, Dry. Technol. **33**, 757 (2014), https://doi.org/10.1080/07373937.2014.990566

[28] A. Baldelli, R.M. Power, R.E.H. Miles, J.P. Reid, and R. Vehring, Effect of crystallization kinetics on the properties of spray dried microparticles,

Aerosol Sci. Tech. **50**, 693 (2016), https://doi.org/10.1080/02786826.2016.1177163

[29] G. Karapetsas, Ch.K. Sahu, and O.K. Matar, Evaporation of sessile droplets laden with particles and insoluble surfactants, Langmuir **32**, 6871 (2016), https://doi.org/10.1021/acs.langmuir.6b01042

[30] S.A. Bakhramov, A.M. Kokhkharov, and U.K. Makhmanov, Thin semiconductor films of fullerene C_{70} nanoaggregates on the surface of a plane glass substrate, Appl. Sol. Energ. **54**, 164 (2018), https://doi.org/10.3103/S0003701X18030052

[31] Y. Yu. Tarasevich, I.V. Vodolazskaya, and O.P. Isakova, Desiccating colloidal sessile drop: dynamics of shape and concentration, Colloid Polym. Sci. **289**, 1015 (2011), https://doi.org/10.1007/s00396-011-2418-8

[32] M.V. Shuba, A.G. Paddubskaya, A.O. Plyushch, P.P. Kuzhir, G.Ya. Slepyan, S.A. Maksimenko, V.K. Ksenevich, P. Buka, D. Seliuta, I. Kasalynas, J. Macutkevic, G. Valusis, C. Thomsen, and A. Lakhtakia, Experimental evidence of localized plasmon resonance in composite materials containing single-wall carbon nanotubes, Phys. Rev. B **85**, 165435 (2012), https://doi.org/10.1103/PhysRevB.85.165435

[33] Y. Tsoumpas, S. Dehaeck, A. Rednikov, and P. Colinet, Effect of Marangoni flows on the shape of thin sessile droplets evaporating into air, Langmuir **31**, 13334 (2015), https://doi.org/10.1021/acs.langmuir.5b02673

[34] R.E.H. Miles, J.F. Davies, and J.P. Reid, The influence of the surface composition of mixed monolayer films on the evaporation coefficient of water, Phys. Chem. Chem. Phys. **18**, 19847 (2016), https://doi.org/10.1039/C6CP03826C

[35] M. Eslamian, Spray-on thin film PV solar cells: advances, potentials and challenges, Coatings **4**, 60 (2014), https://doi.org/10.3390/coatings4010060

[36] J. Važgėla, M. Stephen, G. Juška, K. Genevičius, and K. Arlauskas, Charge carrier transport properties in ternary Si-PCPDTBT:P3HT:PCBM solar cells, Lith. J. Phys. **57**, 37 (2017), https://doi.org/10.3952/physics.v57i1.3454

[37] T. Yakhno, A. Sanin, R. Ilyazov, G. Vildanova, R. Khamzin, N. Astascheva, M. Markovsky, V. Bashirov, and V.J. Yakhno, Drying drop technology as a possible tool for detection leukemia and tuberculosis in cattle, Biomed. Sci. Eng. **8**, 1 (2015), https://doi.org/10.4236/jbise.2015.81001

[38] M.T.A. Rajabi and M. Sharifzadeh, 'Coffee ring effect' in ophthalmology: 'anionic dye deposition' hypothesis explaining normal lid margin staining, Medicine **95**, e3137 (2016), https://doi.org/10.1097/MD.0000000000003137

[39] L. Lanotte, D. Laux, B. Charlot, and M. Abkarian, Role of red cells and plasma composition on blood sessile droplet evaporation, Phys. Rev. E **96**, 053114 (2017), https://doi.org/10.1103/PhysRevE.96.053114

[40] J. Park and J. Moon, Control of colloidal particle deposit patterns within picoliter droplets ejected by ink-jet printing, Langmuir **22**, 3506 (2006), https://doi.org/10.1021/la053450j

[41] F. Hoeng, J. Bras, E. Gicquel, G. Krosnicki, and A. Denneulin, Inkjet printing of nanocellulose–silver ink onto nanocellulose coated cardboard, RSC Adv. **7**, 15372 (2017), https://doi.org/10.1039/C6RA23667G

[42] X. Ye and L. Qi, Two-dimensionally patterned nanostructures based on monolayer colloidal crystals: Controllable fabrication, assembly, and applications, Nano Today **6**, 608 (2011), https://doi.org/10.1016/j.nantod.2011.10.002

[43] V. Lotito and T.J. Zambelli, Self-assembly and nanosphere lithography for large-area plasmonic patterns on graphene, Colloid Interface Sci. **447**, 202 (2015), https://doi.org/10.1016/j.jcis.2014.11.007

[44] U.K. Makhmanov, A.M. Kokhkharov, and S.A. Bakhramov, Organic fractal nano-dimensional structures based on fullerene C_{60}, Fuller. Nanotub. Car. N. **27**, 273 (2019), https://doi.org/10.1080/1536383X.2019.1570922

[45] L.A. Bulavin, I.I. Adamenko, V.M. Yashchuk, T.Yu. Ogul'chansky, Yu.I. Prylutskyy, S.S. Durov, and P. Scharff, Self-organization C_{60} nanoparticles in toluene solution, J. Mol. Liq. **93**, 187 (2001), https://doi.org/10.1016/S0167-7322(01)00228-8

[46] U.K. Makhmanov, O.B. Ismailova, A.M. Kokhkharov, E.A. Zakhidov, and S.A. Bakhramov, Features of self-aggregation of C_{60} molecules in toluene prepared by different methods, Phys. Lett. A **380**, 2081 (2016), https://doi.org/10.1016/j.physleta.2016.04.030

[47] R.V. Bemasson, E. Bienvenue, M. Dellinger, S. Leac, and P. Seta, C_{60} in model biological systems. A visible-UV absorption study of solvent-dependent parameters and solute aggregation, J. Phys. Chem. **98**, 3492 (1994), https://doi.org/10.1021/j100064a035

[48] Yu. Prilutski, S. Durov, L. Bulavin, V. Pogorelov, Y. Astashkin, V. Yashchuk, T. Ogul'chansky, E. Buzaneva, and G. Andrievsky, Study of structure of colloidal particles of fullerenes in water solution, Mol. Cryst. Liq. Cryst. **324**, 65 (1998), https://doi.org/10.1080/10587259808047135

[49] S. Karpitschka, F. Liebig, and H. Riegler, Marangoni contraction of evaporating sessile droplets of binary mixtures, Langmuir **33**, 4682 (2017), https://doi.org/10.1021/acs.langmuir.7b00740

SAVITVARKIŲ C_{60} DARINIŲ FORMAVIMASIS TIRPALE IR KOLOIDINIO TIRPALO GARUOJANČIO LAŠO TŪRYJE

U.K. Makhmanov [a], A.M. Kokhkharov [a], S.A. Bakhramov [a], D. Erts [b]

[a] *Uzbekistano mokslų akademijos Jonų plazmos ir lazerinių technologijų institutas, Taškentas, Uzbekistanas*

[b] *Latvijos universiteto Cheminės fizikos institutas, Ryga, Latvija*